Density Functional Studies of Iron(III) Porphines and Their One-Electron-Oxidized Derivatives

David H. Jones, A. Scott Hinman,* and Tom Ziegler*

Department of Chemistry, The University of Calgary, Calgary, Alberta, Canada T2N 1N4

Received May 4, 1992

The relative energies of selected states for one-electron-oxidized difluoro(porphinato)iron(III) and fluoro(porphinato)-iron(III) have been studied using approximate density functional methods. For the difluoro derivative an iron(IV) (S = 1) state is stabilized relative to an iron(III) A_{2u} π-cation-radical (S = 3) state. For the monofluoro species this ordering of states is reversed. The molecular structures of difluoro(porphinato)iron(III) and the corresponding iron(IV) and iron(III) A_{2u} π-cation-radical species have been investigated using a full geometry optimization. The A_{2u} π-cation-radical species has a geometry very similar to the parent compound. In contrast, the iron(IV) derivative displays significantly shortened Fe–N and Fe–F bond distances. A possible relationship between iron(III) spin state and the site of one-electron oxidation in iron(III) porphyrins is rationalized in terms of exchange energy stabilization and the σ- and π-donor properties of the axial ligand(s). The $\pi \rightarrow \pi^*$ singlet transition energies of chloro(porphinato)-iron(III) have been calculated. Good agreement with experimental values is found, and an assignment of the Q-band region as arising from $14a_1 \rightarrow 18e$ ($a_{2u} \rightarrow e_g^*$) and $5a_2 \rightarrow 18e$ ($a_{1u} \rightarrow e_g^*$) transitions is proposed. The B-band (Soret) region is suggested to arise from $8b_1 \rightarrow 18e$ ($b_{2u} \rightarrow e_g^*$) and $13a_1 \rightarrow 18e$ ($a_{2u}' \rightarrow e_g^*$) transitions.

Introduction

Iron porphyrins have been extensively studied from both experimental and theoretical standpoints partly because of their importance as models for heme enzymes such as cytochromes P-450 or peroxidases. In particular, the one- and two-electron oxidations of ferric porphyrins to form "high-valent" iron(IV) porphyrin analogues of oxidized forms of these enzymes received intense interest from researchers in recent years.[1]

As part of a study on the types of axial ligation which would stabilize an iron(IV) porphyrin relative to the corresponding iron-(III) porphyrin π-cation radical, we have examined one-electron-oxidized iron porphyrin systems using approximate density functional theoretical methods. Our aim was to obtain useful information regarding the structure and relative stabilities of these oxidized iron porphyrins which might enable the important factors influencing their generation to be identified.

Additionally, we have sought to characterize the low-energy electronic transitions of the parent iron(III) porphyrin complexes using the density functional model. Our intent was to examine this important class of compounds using an alternative model to the ab initio[2] and INDO/CI[3] methods currently employed to study these systems.

Computational Details

The reported calculations were all carried out by utilizing the HFS–LCAO program system developed by Baerends et al.[4,5] and vectorized by Ravenek.[5b] The numerical integration procedure applied for the calculations was developed by Becke.[6] All molecular structures were optimized within the C_{2v}-symmetry group. The geometry optimization procedure was based on the method developed by Versluis and Ziegler.[7] An uncontracted triple-ζ STO basis set was employed for iron, whereas the ligand atoms were represented by a double-ζ STO basis set. The $1s^2 2s^2 2p^6$ configuration on Fe and the $1s^2$ configuration on C and N were assigned to the core and treated by the frozen-core approximation.[4] A set of auxiliary[8] s, p, d, f, and g STO functions centered on all nuclei was used in order to fit the molecular density and to present the Coulomb and exchange potentials accurately in each SCF cycle. Geometry optimizations and SCF calculations were based on the local density approximation (LDA)[9] in the representation given by Vosko et al.[10] Energy differences were calculated by including nonlocal corrections to exchange[11] and correlation.[12]

Results and Discussion

(a) Relative Energies of Selected States of One-Electron-Oxidized Iron(III) Porphines with One and Two Fluoride Anions as Axial Ligands. The relative energies for the three lowest states of one-electron-oxidized fluoroiron(III) porphines are shown in Table I. For the difluoro species it is seen that the lowest energy state corresponds to a low-spin (S = 1) iron(IV) species. Formation of a high-spin (S = 3) A_{2u} π-cation radical requires an additional 0.57 eV. An intermediate-spin (S = 2) A_{2u} π-cation radical is 0.74 eV less stable than the iron(IV) porphyrin. In contrast, the lowest energy state for the monofluoroiron(III) porphine cation is the high-spin (S = 3) A_{2u} π-cation radical, which lies 0.70 eV below the iron (IV) (S = 1) state and 1.09 eV below a high-spin (S = 3) A_{1u} π-cation radical.

The results suggest that one-electron oxidation of the isolated difluoroiron(III) porphine anion should be metal-centered, producing an iron(IV) species, whereas a monofluoroiron(III) porphine should produce an iron(III) porphyrin π-cation radical. Therefore a crossover point in the relative stabilities of the two oxidized states is found which depends upon the nature of the axial ligation. Axial ligation to iron(III) porphyrins by one fluoride anion results in π-cation-radical formation on one-electron

* To whom correspondence should be addressed.

(1) (a) Loew, G. H. In *Iron Porphyrins*; Lever, A. B. P., Gray, H. B., Eds.; Addison-Wesley: Reading, MA, 1983; Part I, p 89. (b) Tabushi, I. *Coord. Chem. Rev.* **1988**, *86*, 1. (c) Andersson, L. A.; Dawson, J. H. *Struct. Bonding (Berlin)* **1991**, *74*, 1.
(2) Rawlings, D. C.; Gouterman, M.; Davidson, E. R.; Feller, D. *Int. J. Quantum Chem.* **1985**, *28*, 823.
(3) (a) Edwards, W. D.; Weiner, B.; Zerner, M. C. *J. Phys. Chem.* **1988**, *92*, 6188. (b) Du, P.; Axe, F. U.; Loew, G. H.; Canuto, S.; Zerner, M. C. *J. Am. Chem. Soc.* **1991**, *113*, 8614.
(4) Baerends, E. J.; Ellis, D. E.; Ros, P. *Chem. Phys.* **1973**, *2*, 41.
(5) (a) Baerends, E. J. Ph.D. Thesis, Vrije Universiteit, 1975. (b) Ravenek, W. In *Algorithms and Applications on Vector and Parallel Computers*; Riele, H. J. J., Dekker, Th. J., van de Vorst, H. A., Eds.; Elsevier: Amsterdam, 1987.
(6) Becke, A. D. *J. Chem. Phys.* **1988**, *88*, 2547.
(7) Versluis, L.; Ziegler, T. *J. Chem. Phys.* **1988**, *88*, 322.
(8) Krijn, J.; Baerends, E. J. Fit functions in the HFS-method. Internal Report (in Dutch); Free University: Amsterdam, The Netherlands, 1984.
(9) Gunnarsson, O.; Lundquist, I. *Phys. Rev.* **1974**, *B10*, 1319.
(10) Vosko, S. J.; Wilk, L.; Nusair, M. *Can. J. Phys.* **1980**, *58*, 1200.
(11) Becke, A. D. *Phys. Rev.* **1988**, *A38*, 2398.
(12) Perdew, J. P. *Phys. Rev.* **1986**, *B33*, 8822. Perdew, J. P. *Phys. Rev.* **1986**, *B34*, 7406 (erratum).

0020-1669/93/1332-2092$04.00/0

Table I. Selected States of One-Electron-Oxidized Iron(III) Porphines, [Fe(p)]X

	configuration							energy
	a_{1u}	a_{2u}	$d_{x^2-y^2}$	d_{z^2}	d_{xz}	d_{yz}	d_{xy}	(eV)
				[Fe(p)]F_2				
Fe(IV), $S = 1$	2	2	0	0	1	1	2	0.00
Fe(III) A_{2u} radical, $S = 3$	2	1	1	1	1	1	1	0.57
Fe(III) A_{2u} radical, $S = 2$	2	1	0	1	1	1	2	0.74
				[Fe(p)]F^+				
Fe(III) A_{2u} radical, $S = 3$	2	1	1	1	1	1	1	0.00
Fe(IV), $S = 1$	2	2	0	0	1	1	2	0.70
Fe(III) A_{1u} radical, $S = 3$	1	2	1	1	1	1	1	1.09

oxidation, as predicted.[13,14] Difluoro(tetraphenylporphinato)-iron(III) was originally thought to produce an iron(IV) species on one-electron oxidation;[15] however, more recent experimental work suggests that the immediate electrode product is actually a π-cation radical.[14]

One source of the difference between the experimental observations and the predictions of density functional theory may be a matrix effect. The difluoro(tetraphenylporphinato)iron-(III) anion is produced experimentally by adding tetrabutylammonium fluoride trihydrate to a dichloromethane solution of the monofluoroiron(III) porphyrin.[14,15] It is likely therefore that hydrogen-bonding between fluoride and water is important in these experiments. Support for this argument is provided by the crystal structure of the 2-methylimidazolium salt of the difluoro-(tetraphenylporphinato)iron(III) anion.[16] This contains quasi-linear hydrogen-bonded chains in which the 2-methylimidazolium cation is hydrogen-bonded to two fluoride ions of two adjacent difluoro(tetraphenylporphinato)iron(III) anions. The suggested effect of this hydrogen-bonding is a reduction in the donor properties of the fluoride anion relative to the isolated theoretical system. This reduction in donicity would be expected to favor formation of a high-spin iron(III) porphyrin π-cation radical over formation of a low-spin iron(IV) porphyrin for reasons which will be discussed below. In addition, it should be noted that the iron(III) porphyrin π-cation radical and the iron(IV) porphyrin have quite different electronic structures. Therefore, it may also be possible that the present level of approximate DFT is unable to account for the difference in electron correlation between the two oxidized systems.

(b) Molecular Structures of One-Electron-Oxidized Difluoroiron(III) Porphines. A full geometry optimization was carried out on the high-spin difluoro(porphinato)iron(III) anion, [Fe^{III}(p)]F_2^-, and the corresponding one-electron-oxidized low-spin iron(IV) species, [Fe^{IV}(p)]F_2, as well as the high-spin A_{2u} π-cation-radical species, [Fe^{III}(p$^\bullet$)]F_2. The system of nomenclature adopted for this work is shown in Figure 1. Selected geometrical parameters calculated for these systems are compared with the crystallographic geometry of difluoro(tetraphenylporphinato)iron(III)[16] in Table II. For the difluoro(porphinato)-iron(III) anion, the calculated geometry is in good agreement with the crystallographic geometry of the derivative difluoroiron-(III) tetraphenylporphyrin system. The tendency for local density functional methods to underestimate bond distances has been noted.[17]

The calculated geometry of the high-spin A_{2u} π-cation radical is not significantly different from that of the parent anion. In particular, the Fe–N and Fe–F bond distances are not strongly affected by the removal of an electron from the porphyrin ligand.

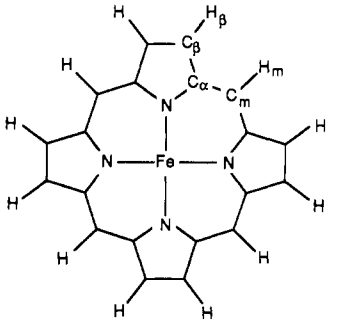

Figure 1. Nomenclature for iron(III) porphines adopted in this work.

Table II. Calculated Geometrical Parameters for Selected Difluoroiron Porphines

	Bond Distances (Å)			
	[Fe^{III}(p)]F_2^-	[Fe^{IV}(p)]F_2	[Fe^{III}(p$^\bullet$)]F_2	[Fe^{III}(tpp)]F_2^- [a]
Fe–F	1.923	1.793	1.912	1.966
Fe–N	2.013	1.953	2.022	2.064
N–C_α	1.374	1.391	1.373	1.377
C_α–C_β	1.423	1.415	1.426	1.441
C_α–C_m	1.368	1.363	1.375	1.403
C_β–C_β	1.355	1.355	1.352	1.341
C_β–H	1.082	1.080	1.093	
C_m–H	1.090	1.084	1.093	
	Bond Angles (Å)			
	[Fe^{III}(p)]F_2^-	[Fe^{IV}(p)]F_2	[Fe^{III}(p$^\bullet$)]F_2	[Fe^{III}(tpp)]F_2^- [a]
Fe–N–C_α	126.1	127.0	126.2	126.0
C_α–N–C_α	107.9	105.9	107.5	107.6
N–C_α–C_β	108.4	109.2	108.6	108.5
N–C_α–C_m	126.8	127.2	126.0	125.9
C_α–C_m–C_α	124.3	121.3	125.3	125.5
C_α–C_β–C_β	107.7	107.8	107.6	107.8
C_α–C_β–H	124.4	124.1	124.5	
C_α–C_m–H	117.8	119.3	117.3	

[a] Averaged values calculated from crystallographic data.[16]

This result is in agreement with crystallographic data of isolated iron(III) porphyrin π-cation radicals.[18] These systems all have Fe–N and Fe–X (X = axial ligand) bond distances which are similar to those in the parent high-spin iron(III) complexes. Interestingly, the optimized high-spin A_{2u} π-cation-radical system showed no inclination to adopt a "saddle"-type ring conformation displayed by a number of porphyrin π-cation radicals in the solid state.[18,19] The difference in energy between the planar porphyrin ring and the saddle conformation was calculated to be only 0.65 eV. However, a geometry optimization performed on the A_{2u} π-cation-radical state starting with a saddle-type structure relaxed back to a planar geometry. Thus, it would appear that a saddle conformation for A_{2u} porphine π-cation radicals would not be expected on the basis of purely electronic considerations and that steric[20] and perhaps solid-state effects[19] are more likely reasons for its observation in the crystal. This result is reasonable since the saddle distortion of the porphyrin π-electron conjugated system acts to decrease the overlap between p orbitals on the C_α and C_m centers. This tends to raise the energy of the π electrons in the porphine π-cation radical.

The calculated geometry for the difluoroiron(IV) porphine differed from those of the parent anion and the A_{2u} π-cation radical in that the Fe–N and Fe–F bond distances were shorter by ca. 0.1 Å (Table II). From crystal field considerations it would be expected that shorter iron–ligand bond distances would help stabilize the low-spin Fe(IV) state. In contrast, the high-spin Fe(III) moiety present in the π-cation-radical state should

(13) Phillippi, M. A.; Shimomura, E. T.; Goff, H. M. *Inorg. Chem.* **1981**, *20*, 1322.
(14) Jones, D. H.; Hinman, A. S. Manuscript submitted for publication.
(15) (a) Hickman, D. L.; Goff, H. M. *Inorg. Chem.* **1983**, *22*, 2789. (b) Hickman, D. L.; Nanthakumar, A.; Goff, H. M. *J. Am. Chem. Soc.* **1988**, *110*, 6384.
(16) Scheidt, W. R.; Lee, Y. J.; Tamai, S.; Hatano, K. *J. Am. Chem. Soc.* **1983**, *105*, 778.
(17) Ziegler, T. *Chem. Rev.* **1991**, *91*, 651.
(18) Gans, P.; Buisson, G.; Duee, E.; Marchon, J.-C.; Erler, B. S.; Scholz, W. F.; Reed, C. A. *J. Am. Chem. Soc.* **1986**, *108*, 1223.
(19) Scheidt, W. R.; Lee, Y. J. *Struct. Bonding (Berlin)* **1987**, *64*, 1.
(20) Barkigia, K. M.; Berber, M. D.; Fajer, J.; Medforth, C. J.; Renner, M. W.; Smith, K. M. *J. Am. Chem. Soc.* **1990**, *112*, 8851.

Table III. Relationship between Spin State and Site of Redox in Ferric Porphyrins

complex	spin state	redox site	1e-oxidized product	ref
[Fe(tpp)]F	$^5/_2$	P	[Fe(tpp)]F(ClO_4)	13, 14
[Fe(tpp)]Cl	$^5/_2$	P	[Fe(tpp)]Cl($SbCl_6$)	18
[Fe(tpp)]Br	$^5/_2$	P	[Fe(tpp)]Br(ClO_4)	13
[Fe(tpp)]I	$^5/_2$	P	[Fe(tpp)]I(ClO_4)	13
[Fe(tmp)]OH	$^5/_2$	P	[Fe(tmp)]OH(PF_6)	22
[Fe(tpp)]F_2^-	$^5/_2$	P	[Fe(tpp)]F_2	14
[Fe(tpp)]$_2$O	$^5/_2$	P	[Fe(tpp)]$_2$O(ClO_4)	23
[Fe(tpp)](NO_3)	$^5/_2$	P	[Fe(tpp)](NO_3)-(ClO_4)	13
[Fe(tpp)](OC_6H_5)	$^5/_2$	P	[Fe(tpp)](OC_6H_5)-(ClO_4)	13
[Fe(tpp)]NCS	$^5/_2$	P	[Fe(tpp)]NCS(ClO_4)	13
[Fe(tpp)](ClO_4)	$^5/_2$, $^3/_2$	P	[Fe(tpp)](ClO_4)$_2$	18
[Fe(tpp)]-(OSO_2CF_3)	$^5/_2$, $^3/_2$	P	[Fe(tpp)](OSO_2CF_3)-(ClO_4)	24
[Fe(tmp)]-(OCH_3)$_2^-$	$^1/_2$	M	[Fe(tmp)](OCH_3)$_2$	25, 26
[Fe(tmp)](OH)$_2^-$	$^1/_2$	M	[Fe(tmp)]O + H_2O	26, 27
[Fe(oep)](C_6H_5)	$^1/_2$	M	[Fe(oep)](C_6H_5)-(ClO_4)	28
[Fe(tpp)](C_6F_4H)	$^5/_2$	M?	[Fe(tpp)](C_6F_4H)-(ClO_4)	29
[Fe(tpp)]$_2$N	$^1/_2$	M	[Fe(tpp)]$_2N^+$	30
[Fe(tpp)]$_2C^-$	$^1/_2$?	M	[Fe(tpp)]$_2$C	30a, 31
[Fe(oep)](ImH)$_2$Cl	$^1/_2$	P	[Fe(oep)](ImH)$_2$Cl-(ClO_4)	32

be favored by a weaker crystal field and hence longer iron–ligand bond distances. The shorter metal–ligand bond distances also lend support to the idea that increased covalency in the metal–ligand interaction might help to stabilize the iron(IV) state (vide infra). The available experimental evidence suggests that iron–axial ligand bond distances in low-spin iron(IV) porphyrins are unusually short.[1c] Furthermore, Fe–N bond distances in low-spin Fe(IV) porphyrins[1c] are similar to those observed in low-spin Fe(III) porphyrins but are significantly shorter than those seen in high-spin iron(III) porphyrins.[21]

(c) A Possible Spin-State/Oxidation-Site Relationship in Iron(III) Porphyrins. Given that a clear relationship between spin state and Fe–N and Fe–X bond distances exists for iron(III) porphyrins of a given coordination number[21] and that low-spin Fe(IV) porphyrins and high-spin iron(III) porphyrin π-cation radicals display structural differences (vide supra), it seemed possible that the spin state of iron(III) porphyrins and their site of oxidation might also be related. The assumption underlying this idea is that formal one-electron oxidations of iron(III) porphyrins proceed without significant structural rearrangement and therefore that the properties of the ligand set which favor one oxidized state over another are manifest to some degree in the iron(III) porphyrin precursor. Table III contains a listing of iron(III) porphyrins with various axial ligands, their spin states, the accepted sites of electron transfer on one-electron oxidation (at either the porphyrin ring, P, to form an iron(III) porphyrin π-cation radical, or the central metal, M, to form an iron(IV) porphyrin), and the expected oxidized products. Although the data set is not exhaustive, it is interesting to note that practically all high-spin ($S = ^5/_2$) and quantum-admixed-spin ($S = ^5/_2, ^3/_2$) iron(III) porphyrins are considered to undergo one-electron oxidation to form iron(III) porphyrin π-cation radicals in which Fe(III) probably retains a high or quantum-admixed spin state.[18,24] In contrast, low-spin Fe(III) porphyrins may form either low-spin iron(IV) porphyrins or low-spin iron(III) porphyrin π-cation radicals on one-electron oxidation, depending upon the type of axial ligation.

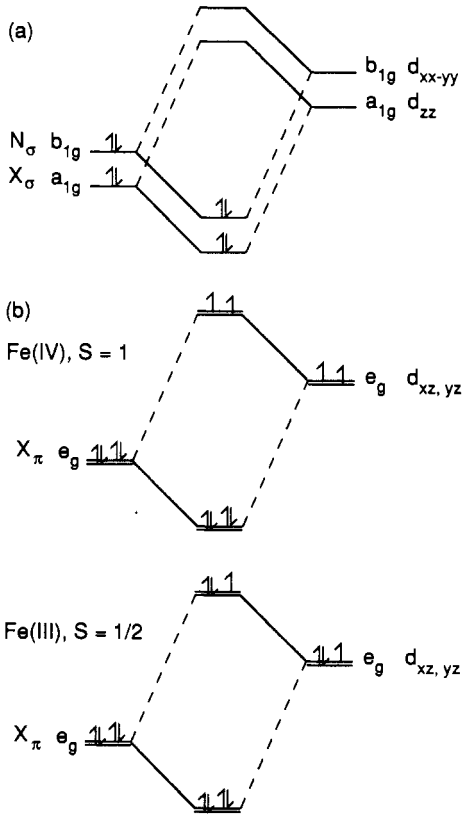

Figure 2. Interaction diagrams showing the effect of increased (a) σ-donation and (b) π-donation by an axial ligand X upon the d-based molecular orbitals for an iron(IV) ($S = 1$) state and an iron(III) ($S = ^1/_2$) state.

The observations outlined above suggest that, in general, spin is preserved on one-electron oxidation of iron(III) porphyrins. Furthermore, it appears that only in the case of low-spin iron(III) porphyrins are the iron(IV) and iron(III) π-cation-radical states both accessible on one-electron oxidation. The driving force for the formation of high-spin iron(III) porphyrin π-cation radicals from high-spin iron(III) precursors may be the retention of an exchange energy stabilization afforded by the high-spin Fe(III) configuration. Since low-spin Fe(IV) porphyrins and low-spin iron(III) porphyrin π-cation radicals have lower spin multiplicities the effects of exchange would be expected to be smaller than for the case of high-spin systems. Accordingly, differences in one-electron energies may be more important in determining the relative stability of the iron(IV) and iron(III) π-cation-radical states. Figure 2 shows interaction diagrams between metal-based d orbitals and axial X ligands as well as the σ orbitals on N. The bottom level in each diagram is primarily represented by the ligand orbital with a small in-phase admixture from the metal-d component. The upper level in each diagram is represented by the metal component with an out-of-phase contribution from the ligand orbital. The energy splitting between the two levels in each diagram increases with the (a) σ- or (b) π-donor ability of the ligand. Since both states possess vacant $d_{x^2-y^2}$ and d_{z^2} orbitals, it appears that increased σ-donation (Figure

(21) Scheidt, W. R.; Reed, C. A. *Chem. Rev.* **1981**, *81*, 543.
(22) Jones, D. H.; Hinman, A. S. Manuscript in preparation.
(23) Phillippi, M. A.; Goff, H. M. *J. Am. Chem. Soc.* **1982**, *104*, 6026.
(24) Boersma, A. D.; Goff, H. M. *Inorg. Chem.* **1984**, *23*, 1671.
(25) Groves, J. T.; Quinn, R.; McMurry, T. J.; Nakamura, M.; Lang, G.; Boso, B. *J. Am. Chem. Soc.* **1985**, *107*, 354.
(26) Swistak, C.; Mu, X. H.; Kadish, K. M. *Inorg. Chem.* **1987**, *26*, 4360.
(27) Czernuszewicz, R. S.; Macor, K. A. *J. Raman Spectrosc.* **1988**, *19*, 552.
(28) Lancon, D.; Cocolios, P.; Guilard, R.; Kadish, K. M. *J. Am. Chem. Soc.* **1984**, *106*, 4472.
(29) Guilard, R.; Boisselier-Cocolios, B.; Tabard, A.; Cocolios, P.; Simonet, B.; Kadish, K. M. *Inorg. Chem.* **1985**, *24*, 2509.
(30) (a) English, D. R.; Hendrickson, D. N.; Suslick, K. S. *Inorg. Chem.* **1983**, *22*, 367. (b) Kadish, K. M.; Rhodes, R. K.; Bottomley, L. A.; Goff, H. M. *Inorg. Chem.* **1981**, *20*, 3195.
(31) (a) Battioni, J. P.; Lexa, D.; Mansuy, D.; Saveant, J.-M. *J. Am. Chem. Soc.* **1983**, *105*, 207. (b) Lancon, D.; Kadish, K. M. *Inorg. Chem.* **1984**, *23*, 3942.
(32) Goff, H. M.; Phillippi, H. M. *J. Am. Chem. Soc.* **1983**, *105*, 7567.

Table IV. Calculated Singlet Transition Energies of Chloro(porphinato)iron(III) ($S = {}^5/_2$)

transition	ΔE (eV)	ΔE_{expt} (eV) [Fe(tpp)]Cl[a]	ΔE_{expt} (eV) [Fe(oep)]Cl[b]
$13a_1 \rightarrow 18e$	3.58		
		3.26 (B)	3.28 (B)
$8b_1 \rightarrow 18e$	3.14		
		2.97 (B)	
$14a_1 \rightarrow 18e$	2.45		2.46 (Q)
		2.42 (Q)	
$5a_2 \rightarrow 18e$	2.38		2.32 (Q)

[a] Taken from ref 23. [b] Taken from ref 34.

2a) would favor both states by about the same amount. In contrast, the effect of increasing π-donation (Figure 2b) is seen to favor low-spin iron(IV) over low-spin Fe(III) since an extra electron is destabilized by this interaction in the low-spin iron(III) case. It has previously been recognized that π-donation from the axial ligand to iron(IV) is important in stabilizing this high-valent state.[1a,c,33]

An apparent exception to the relationship outlined above is the high-spin iron(III) porphyrins with σ-bonded perfluoroaryl axial ligands such as [Fe(tpp)](C_6F_4H) and [Fe(tpp)](C_6F_5).[29] These systems are considered to undergo oxidation centered at iron to form iron(IV) derivatives in a fashion analogous to systems like [Fe(oep)]C_6H_5.[28] From our considerations these high-spin iron(III) porphyrins might be expected to form high-spin iron(III) porphyrin π-cation radicals. In our view, the UV–visible spectral changes accompanying the oxidation of [Fe(tpp)](C_6F_4H) are reminiscent of those which accompany formation of an iron(III) porphyrin π-cation radical.[29] Further spectroscopic characterization of the oxidized species formed in these reactions would be useful in clarifying this question.

(d) $\pi \rightarrow \pi^*$ Singlet Transition Energies of Chloro(porphinato)iron(III). The calculated $\pi \rightarrow \pi^*$ singlet transition energies of chloro(porphinato)iron(III) are shown in Table IV together with experimental values for two widely-studied iron(III) porphyrin complexes.[23,34] The UV–visible spectra of iron porphyrins generally display an intense absorption close to 3.2 eV, known as the B-band or Soret band, and two weaker transitions near 2.4 eV, known as the Q-bands (see Figure 3). All these transitions display x,y-polarization. The calculated values are consistent with the assignment of the Q-band region as arising from $14a_1 \rightarrow 18e$ ($a_{2u} \rightarrow e_g^*$) and $5a_2 \rightarrow 18e$ ($a_{1u} \rightarrow e_g^*$) transitions. The B-band (Soret) region is suggested to arise from $8b_1 \rightarrow 18e$ ($b_{2u} \rightarrow e_g^*$) and $13a_1 \rightarrow 18e$ ($a_{2u}' \rightarrow e_g^*$) transitions. The $\pi \rightarrow \pi^*$ transitions shown in Table IV are of E_u symmetry (x,y-polarized) and fully allowed. Furthermore, since they arise from electronic transitions within the porphyrin π-system they would be expected to be more intense than charge-transfer or d–d transitions involving the paramagnetic iron center and hence dominate the observed spectrum. Unfortunately, we are unable to calculate intensities for the $\pi \rightarrow \pi^*$ transitions in Table IV.

The present interpretation of the UV–visible spectrum of chloro(porphinato)iron(III) provides an alternative explanation to the popular four-orbital model proposed by Gouterman (see Figure 2).[35] This model is based on an idea that the two highest filled porphyrin π molecular orbitals of a_{1u} and a_{2u} symmetries are accidentally degenerate and that electronic transitions from these orbitals to the lowest unoccupied e_g^* level are consequently heavily mixed and produce an allowed B-state and a formally disallowed Q-state. A major success of this model is its ability to explain the large difference in intensity between the Q- and B-bands. The four-orbital model has been used to interpret a substantial body of experimental data based on UV, CD, MCD, and vibrational spectroscopy.[3,35,36]

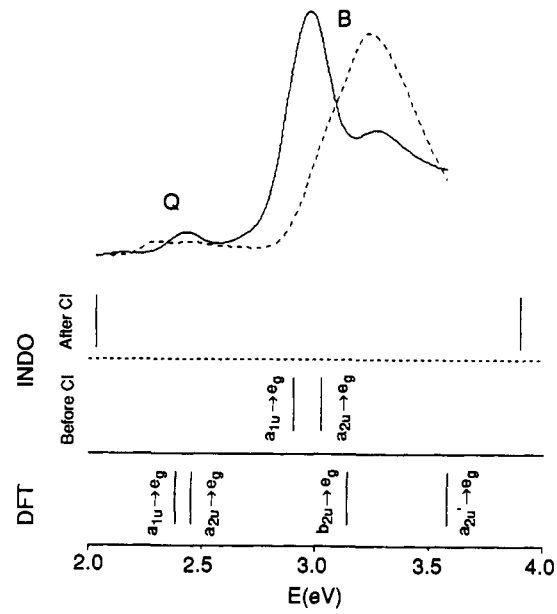

Figure 3. Comparison of calculated transition energies using INDO/CI methods (taken from ref 3a) based on Gouterman's four-orbital model and HFS–LCAO methods (present work). The experimental spectra are those due to chloro(tetraphenylporphinato)iron(III) (solid line) and chloro(octaethylporphinato)iron(III) (dashed line).

Another point of interest is the origin of the two Q-bands. The four-orbital model predicts only one electronic transition in this energy range, and the second band has been suggested to arise from vibrational–electronic coupling.[38] In our alternative interpretation, the two bands arise from two different electronic transitions. We hope to explore the reinterpretation of the Q- and B-bands as programs for the simulation of UV intensities as well as CD and MCD spectra become available within the density functional (DF) formalism. At the moment, our interpretation rests solely on the good agreement between our calculated excitation energies and experiment as well as the strong track record of DF theory in connection with the assignment of electronic spectra.[17] Our reassignment must thus be considered as tentative and in no way conclusive.

Acknowledgment. We wish to thank the Natural Sciences and Engineering Research Council of Canada for financial support.

(33) Balch, A. L.; Renner, M. W. *J. Am. Chem. Soc.* **1986**, *108*, 2603.
(34) Fleischer, E. B.; Palmer, J. M.; Srivastava, T. S.; Chatterjee, A. *J. Am. Chem. Soc.* **1971**, *93*, 3162.
(35) Gouterman, M. *J. Mol. Spectrosc.* **1961**, *6*, 138.
(36) Weiss, C.; Kobayashi, H.; Gouterman, M. *J. Mol. Spectrosc.* **1965**, *16*, 415.
(37) Edwards, W. D.; Zerner, M. C. *Can. J. Chem.* **1985**, *63*, 1763.
(38) (a) Eaton, W. A.; Hochstrasser, R. M. *J. Chem. Phys.* **1967**, *46*, 2533. (b) Eaton, W. A.; Hochstrasser, R. M. *J. Chem. Phys.* **1968**, *49*, 985.